

# Husimi function and phase-space analysis of bilayer quantum Hall systems at $\nu = 2/\lambda$

M. Calixto and C. Peón-Nieto

*Departamento de Matemática Aplicada and Instituto "Carlos I" de Física Teórica y Computacional,  
Universidad de Granada, Fuentenueva s/n, 18071 Granada, Spain*

(Dated: June 20, 2022)

We propose localization measures in phase space of the ground state of bilayer quantum Hall (BLQH) systems at fractional filling factors  $\nu = 2/\lambda$ , to characterize the three quantum phases (shortly denoted by spin, canted and ppin) for arbitrary  $U(4)$ -isospin  $\lambda$ . We use a coherent state (Bargmann) representation of quantum states, as holomorphic functions in the 8-dimensional Grassmannian phase-space  $\mathbb{G}_2^4 = U(4)/[U(2) \times U(2)]$  (a higher-dimensional generalization of the Haldane's 2-dimensional sphere  $\mathbb{S}^2 = U(2)/[U(1) \times U(1)]$ ). We quantify the localization (inverse volume) of the ground state wave function in phase-space throughout the phase diagram (i.e., as a function of Zeeman, tunneling, layer distance, etc, control parameters) with the Husimi function second moment, a kind of inverse participation ratio that behaves as an order parameter. Then we visualize the different ground state structure in phase space of the three quantum phases, the canted phase displaying a much higher delocalization than the spin and ppin phases, where the ground state is highly coherent. We find a good agreement between analytic (variational) and numeric diagonalization results.

PACS numbers: 73.43.-f, 73.43.Nq, 73.43.Jn, 71.10.Pm, 03.65.Fd, 89.70.Cf

## I. INTRODUCTION

Information theoretic and statistical measures have proved to be useful in the description and characterization of quantum phase transitions (QPTs). For example, in the traditional Anderson metal-insulator transition [1–5], Hamiltonian eigenfunctions underlie strong fluctuations. Also, the localization of the electronic wave function can be regarded as the key manifestation of quantum coherence at a macroscopic scale in a condensed matter system. In this article we want to analyze QPTs in BLQH systems at fractional filling factors  $\nu = 2/\lambda$  from an information theoretic perspective. The integer case  $\nu = 2$  has been extensively studied in the literature (see e.g. [6–12]), where the analysis of the ground state structure reveals the existence of (in general) three quantum phases, shortly denoted by: spin, canted and ppin [6, 7], depending on which order parameter (spin or pseudospin/layer) dominates across the control parameter space: tunneling, Zeeman, bias voltage, etc, couplings. Here we shall study localization properties in phase-space of the ground state in each of the three quantum phases for arbitrary  $\lambda$  (number of magnetic flux quanta per electron). For it, we shall use a phase-space representation  $\langle Z|\psi\rangle = \psi(Z)$  of quantum states  $|\psi\rangle$ , where  $|Z\rangle$  denotes an arbitrary coherent (minimal uncertainty) state labeled by points  $Z \in \mathbb{G}_2^4 = U(4)/[U(2) \times U(2)] \simeq \text{Mat}_{2 \times 2}(\mathbb{C})$ , the complex Grassmannian with complex dimension 4. The Grassmannian  $\mathbb{G}_2^4$  can be seen as a higher-dimensional generalization of the Haldane's sphere  $\mathbb{S}^2 = U(2)/[U(1) \times U(1)]$  [13] for monolayer fractional QH systems, with  $Z$  a  $2 \times 2$  matrix generalization of the stereographic projection  $z = \tan(\theta/2)e^{i\phi}$  of a point  $(\theta, \phi)$  (polar and azimuthal angles) of the Riemann sphere  $\mathbb{S}^2$  onto the complex plane. Standard spin- $s$  coherent states (CS) on the sphere  $\mathbb{S}^2 = \mathbb{C}P^1$  (isomorphic to the complex projec-

tive space) are very well known (see traditional references [14–17] on CS). Its extension to the complex projective  $\mathbb{C}P^{N-1} = U(N)/[U(N-1) \times U(1)]$  (the symmetric case) is quite straightforward and  $\mathbb{C}P^{N-1}$  is related to the phase space of  $N$ -component QH systems at fractional values of  $\nu = 1$ . The case  $1 < \nu < N/2 + 1$  is much more involved and the phase space is in this case the complex Grassmannian  $\mathbb{G}_M^N = U(N)/[U(M) \times U(N-M)]$ . The 4-component (spin-layer) CS on  $\mathbb{G}_2^4$  for fractional values  $\nu = 2/\lambda$  of  $\nu = 2$  have been introduced in [18–20] and recently extended to the  $N$ -component case  $\mathbb{G}_M^N$  for filling factors  $\nu = M/\lambda$  in [21]. In [22] we have used these CS as variational states to study the classical limit and phase diagram of BLQH systems. Here we are interested in the CS (phase-space or Bargmann) representation  $\langle Z|\psi\rangle = \psi(Z)$  of quantum states  $|\psi\rangle$ , the squared norm  $Q_\psi(Z) = |\psi(Z)|^2$  being a positive quasi-probability distribution called the Husimi or  $Q$ -function. Both, Husimi and Wigner, phase-space quasi-probability distributions are useful to characterize phase-space properties of many quantum systems, specially in Quantum Optics [23], although Husimi proves sometimes to be more convenient because, unlike Wigner, it is non-negative. It can also be measured by tomographic, spectroscopic, interferometric, etc, techniques. For example, one can visualize the time evolution of CS of light in a Kerr medium by measuring  $Q_\psi$  by cavity state tomography [24]. Moreover, the zeros of the Husimi function have been used as an indicator of the regular or chaotic behavior in quantum maps for a variety of atomic, molecular [25, 26], condensed matter systems [27], etc. Information theoretic measures of  $Q_\psi$  have also been considered as an indicator of metal-insulator [4] and topological-band insulator [28] phase transitions, together with other QPTs in Dicke, vibron, Lipkin-Meshkov-Glick and BEC models [29–33], etc.

Using a CS representation, we shall obtain in this article the Husimi function  $Q_\psi(Z)$  of the ground state  $\psi$  of a BLQH system at  $\nu = 2/\lambda$ . This representation will allow us to visualize the structure of the ground state  $\psi$  in phase-space in each of the three quantum phases (spin, canted and ppin). The Hamiltonian we shall use is an adaptation of the integer  $\nu = 2$  case [6] to the fractional  $\nu = 2/\lambda$  case [22]. The localization of  $\psi$  in phase-space can be quantified by the Husimi function second moment  $M_\psi = \int_{\mathbb{G}_2^4} Q_\psi^2(Z) d\mu(Z)$ , where  $d\mu(Z)$  denotes a proper measure on  $\mathbb{G}_2^4$  (see later). Maximal localization (minimum volume/uncertainty) in phase space is attained when  $\phi$  is itself a CS. This statement is in fact a conjecture that was proved for harmonic oscillator CS [34] and recently for the particular case of  $SU(2)$  spin- $s$  CS [35]. Here we check the validity of this conjecture for Grassmannian  $\mathbb{G}_2^4$  CS. In fact, we obtain that the ground state in spin and ppin phases is highly coherent (maximally localized), whereas it is more delocalized (higher uncertainty) in the canted phase. We also evaluate spin and ppin quantum fluctuations...

The organization of the paper is as follows. In section II we provide an oscillator realization of the  $U(4)$  operators and the Landau-site Hilbert space for  $\nu = 2/\lambda$ . We also introduce the isospin- $\lambda$  coherent states on  $\mathbb{G}_2^4$ , which are essential for the semiclassical ground state analysis of BLQH systems discussed in subsequent sections and to introduce the Husimi function and localization measures in phase space. More details can be found in references [18–20]. In section III we study the Landau-site Hamiltonian governing the BLQH system at  $\nu = 2/\lambda$ , which is an adaptation of the one proposed in [6] for  $\lambda = 1$  to the many body case (arbitrary  $\lambda$ ) and has already been discussed in [22]. Using CS expectation values of the Hamiltonian, we perform a semiclassical analysis and a study of its quantum phases. In section IV we make a variational and exact (numerical diagonalization) ground state analysis and characterize the quantum phases (spin, ppin and canted) using localization measures in phase space. Variational results agree with numerical diagonalization calculations and provide analytical formulas for some physical quantities. The last section is left for conclusions and outlook.

## II. $U(4)$ COHERENT STATES AND HUSIMI FUNCTION

### A. $U(4)$ symmetry and bosonic flux quanta representation

BLQH systems underlie an isospin  $U(4)$  symmetry. In order to emphasize the spin  $SU(2)$  symmetry in the, let us say, bottom  $b$  (pseudospin down) and top  $a$  (pseudospin up) layers, it is customary to denote the  $U(4)$  generators in the four-dimensional fundamental representation by the sixteen  $4 \times 4$  matrices  $\tau_{\mu\nu} \equiv \sigma_\mu^{\text{ppin}} \otimes \sigma_\nu^{\text{spin}}$ ,  $\mu, \nu = 0, 1, 2, 3$ , where  $\sigma_\mu$  denote the usual Pauli

matrices  $\sigma_k, k = 1, 2, 3$ , plus the identity  $\sigma_0$ . In the fractional case, bosonic magnetic flux quanta are attached to the electrons to form composite fermions [36]. Let us denote by  $(a_l^\dagger)^\dagger$  [resp.  $(b_l^\dagger)^\dagger$ ] creation operators of magnetic flux quanta (flux quanta in the sequel) attached to the electron  $l$  with spin down [resp. up] at layer  $a$  [resp.  $b$ ], and so on. For the case of two electrons,  $l = 1, 2$ , the four-component electron “field”  $\zeta$  is arranged as a compound  $\zeta = (\zeta_1, \zeta_2)$  of two fermions, so that the sixteen  $U(4)$  density operators are then written as bilinear products of creation and annihilation operators as (the so called Schwinger oscillator realization) and E. Pérez-Romero

$$T_{\mu\nu} = \text{tr}(\zeta^\dagger \tau_{\mu\nu} \zeta), \quad \zeta = \begin{pmatrix} \mathbf{a} \\ \mathbf{b} \end{pmatrix} = \begin{pmatrix} a_1^\downarrow & a_2^\downarrow \\ a_1^\uparrow & a_2^\uparrow \\ b_1^\downarrow & b_2^\downarrow \\ b_1^\uparrow & b_2^\uparrow \end{pmatrix}. \quad (1)$$

In the BLQH literature (see e.g. [7]) it is customary to denote the total spin  $S_k = T_{0k}/2$  and pseudospin  $P_k = T_{k0}/2$ , together with the remaining 9 isospin  $R_{kl} = T_{lk}/2$  operators for  $k, l = 1, 2, 3$ . A constraint in the Fock space of eight boson modes is imposed such that  $\zeta^\dagger \zeta = \lambda I_2$ , with  $\lambda$  representing the number of magnetic flux lines piercing each electron and  $I_2$  the  $2 \times 2$  identity. In particular, the linear Casimir operator  $T_{00} = \text{tr}(\zeta^\dagger \zeta)$ , providing the total number of flux quanta, is fixed to  $n_a + n_b = \lambda + \lambda = 2\lambda$ , with  $n_a = n_{a1}^\uparrow + n_{a1}^\downarrow + n_{a2}^\uparrow + n_{a2}^\downarrow$  the total number of flux quanta in layer  $a$  (resp. in layer  $b$ ). The quadratic Casimir operator is also fixed to

$$\vec{S}^2 + \vec{P}^2 + \mathbf{R}^2 = \lambda(\lambda + 4). \quad (2)$$

We also identify the interlayer imbalance operator  $P_3$ , which measures the excess of flux quanta between layers  $a$  and  $b$ , that is  $\frac{1}{2}(n_a - n_b)$ . Therefore, the realization (1) defines a unitary bosonic representation of the  $U(4)$  matrix generators  $\tau_{\mu\nu}$  in the Fock space with constraints. This unitary irreducible representation arises in the Clebsch-Gordan decomposition of a tensor product of  $2\lambda$  four-dimensional (fundamental, elementary) representations of  $U(4)$ ; for example, in Young tableau notation:

$$\overbrace{\square \otimes \dots \otimes \square}^{2\lambda} = \overbrace{\begin{array}{|c|c|c|} \hline \dots & \dots & \dots \\ \hline \dots & \dots & \dots \\ \hline \end{array}}^{\lambda} \oplus \dots, \quad (3)$$

or  $\overbrace{[1] \otimes \dots \otimes [1]}^{2\lambda} = [\lambda, \lambda] \oplus \dots$ , where we wanted to highlight rectangular Young tableaux of shapes  $[\lambda, \lambda]$  (2 rows of  $\lambda$  boxes each) corresponding to 2 electrons pierced by  $\lambda$  magnetic flux lines (i.e., fractional filling factor  $\nu = 2/\lambda$ ). These are the Young tableaux determining our carrier Hilbert space  $\mathcal{H}_\lambda(\mathbb{G}_2^4)$  associated to the eight-dimensional Grassmannian phase spaces  $\mathbb{G}_2^4 = U(4)/U(2) \times U(2)$  (see [37–39] for similar pictures in  $N$ -component antiferromagnets). The dimension of this representation can be

calculated by the hook-length formula and gives

$$d_\lambda = \frac{1}{12}(\lambda+1)(\lambda+2)^2(\lambda+3) \quad (4)$$

In references [18, 21] we have also provided a physical argument to derive the expression of  $d_\lambda$  in a composite fermion picture. It turns out to coincide with the total number of ways to distribute  $2\lambda$  flux quanta among two identical electrons in four (spin-pseudospin) states. Note that quantum states associated to Young tableaux  $[\lambda, \lambda]$  are antisymmetric (fermionic character) under the interchange of the two electrons (two rows) for  $\lambda$  odd, whereas they are symmetric (bosonic character) for  $\lambda$  even. Composite fermions require then  $\lambda$  odd.

### B. Orthonormal basis and coherent states

In Refs. [18, 19] we have worked out an orthonormal basis of the  $d_\lambda$ -dimensional carrier Hilbert space  $\mathcal{H}_\lambda(\mathbb{G}_2^4)$ , which is spanned by the set of orthonormal basis vectors

$$B_\lambda(\mathbb{G}_2^4) = \left\{ |j, m\rangle_{q_a, q_b}, \quad \begin{array}{l} 2j, m \in \mathbb{N}, \\ q_a, q_b = -j, \dots, j \end{array} \right\}_{2j+m \leq \lambda}, \quad (5)$$

whose general expression is given by the action of creation operators  $\mathbf{a}^\dagger$  and  $\mathbf{b}^\dagger$  in layers  $a$  and  $b$  acting on the Fock vacuum  $|0\rangle_F$  as

$$\begin{aligned} |j, m\rangle_{q_a, q_b} &= \frac{1}{\sqrt{2j+1}} \sum_{q=-j}^j (-1)^{q_a-q} \quad (6) \\ &\times \frac{\varphi_{-q, -q_a}^{j, m}(\mathbf{a}^\dagger)}{\sqrt{\frac{\lambda!(\lambda+1)!}{(\lambda-2j-m)!(\lambda+1-m)!}}} \frac{\varphi_{q, q_b}^{j, \lambda-2j-m}(\mathbf{b}^\dagger)}{\sqrt{\frac{\lambda!(\lambda+1)!}{m!(2j+m+1)!}}} |0\rangle_F, \end{aligned}$$

where

$$\begin{aligned} \varphi_{q_a, q_b}^{j, m}(Z) &= \sqrt{\frac{2j+1}{\lambda+1}} \binom{\lambda+1}{2j+m+1} \binom{\lambda+1}{m} \quad (7) \\ &\times \det(Z)^m \mathcal{D}_{q_a, q_b}^j(Z), \quad \begin{array}{l} 2j+m \leq \lambda, \\ q_a, q_b = -j, \dots, j, \end{array} \end{aligned}$$

are homogeneous polynomials of degree  $2j+2m$  in four complex variables  $z_{uv} \in \mathbb{C}$  arranged in a  $2 \times 2$  complex matrix  $Z = \begin{pmatrix} z_{11} & z_{12} \\ z_{21} & z_{22} \end{pmatrix}$  (a point on the Grassmannian  $\mathbb{G}_2^4$ ). By  $\mathcal{D}_{q_a, q_b}^j(Z)$  we denote the usual Wigner  $\mathcal{D}$ -matrix [40] with angular momentum  $j$ . They are homogeneous polynomials of degree  $2j$  explicitly given by

$$\begin{aligned} \mathcal{D}_{q_a, q_b}^j(Z) &= \sqrt{\frac{(j+q_a)!(j-q_a)!}{(j+q_b)!(j-q_b)!}} \sum_{k=\max(0, q_a+q_b)}^{\min(j+q_a, j+q_b)} \quad (8) \\ &\binom{j+q_b}{k} \binom{j-q_b}{k-q_a-q_b} z_{11}^k z_{12}^{j+q_a-k} z_{21}^{j+q_b-k} z_{22}^{k-q_a-q_b}. \end{aligned}$$

The set of polynomials (7) verifies the closure relation [18]

$$\sum_{m=0}^{\lambda} \sum_{j=0; \frac{1}{2}}^{(\lambda-m)/2} \sum_{q_a, q_b=-j}^j \overline{\varphi_{q_a, q_b}^{j, m}(Z')} \varphi_{q_a, q_b}^{j, m}(Z) = K_\lambda(Z'^\dagger, Z), \quad (9)$$

with  $K_\lambda(Z'^\dagger, Z) = \det(\sigma_0 + Z'^\dagger Z)^\lambda$  the so called Bergmann kernel. The orthonormal basis states (6) are eigenstates of the following operators:

$$\begin{aligned} P_3 |j, m\rangle_{q_a, q_b} &= (2j+2m-\lambda) |j, m\rangle_{q_a, q_b}, \\ (\vec{S}_a^2 + \vec{S}_b^2) |j, m\rangle_{q_a, q_b} &= 2j(j+1) |j, m\rangle_{q_a, q_b}, \quad (10) \\ S_{\ell 3} |j, m\rangle_{q_a, q_b} &= q_\ell |j, m\rangle_{q_a, q_b}, \quad \ell = a, b, \end{aligned}$$

where we have defined angular momentum operators in layers  $a$  and  $b$  as  $S_{ak} = -\frac{1}{2}(S_k + R_{k3})$  and  $S_{bk} = \frac{1}{2}(S_k - R_{k3})$ ,  $k = 1, 2, 3$ , respectively, so that  $\vec{S}_a^2 + \vec{S}_b^2 = \frac{1}{2}(\vec{S}^2 + \vec{R}_3^2)$ . Therefore,  $j$  is a half-integer representing the total angular momentum of layers  $a$  and  $b$ , whereas  $q_a$  and  $q_b$  are the corresponding third components. The integer  $m$  is related to the interlayer imbalance population (ppin third component  $P_3$ ) through  $\frac{1}{2}(n_a - n_b) = (2j+2m-\lambda)$ ; thus,  $m = \lambda, j = 0$  means  $n_a = 2\lambda$  (i.e., all flux quanta occupying layer  $a$ ), whereas  $m = 0, j = 0$  means  $n_b = 2\lambda$  (i.e., all flux quanta occupying layer  $b$ ). The angular momentum third components  $q_a, q_b$  measure the imbalance between spin up and down in each layer, more precisely,  $q_a = \frac{1}{2}(n_{a1}^\uparrow - n_{a1}^\downarrow + n_{a2}^\uparrow - n_{a2}^\downarrow)$  and similarly for  $q_b$ .

Coherent states on  $\mathbb{G}_2^4$  are defined as boson (magnetic flux quanta) condensates (see [18])

$$|Z\rangle = \frac{1}{\lambda! \sqrt{\lambda+1}} \left( \frac{\det(\check{\mathbf{b}}^\dagger + Z^t \check{\mathbf{a}}^\dagger)}{\sqrt{\det(\sigma_0 + Z^\dagger Z)}} \right)^\lambda |0\rangle_F, \quad (11)$$

where  $\check{\mathbf{a}}^\dagger = \frac{1}{2} \eta^{\mu\nu} \text{tr}(\sigma_\mu \mathbf{a}^\dagger) \sigma_\nu$  denotes the ‘‘parity reversed’’  $2 \times 2$ -matrix creation operator of  $\mathbf{a}^\dagger$  in layer  $a$  (similar for layer  $b$ ) [we are using Einstein summation convention with Minkowskian metric  $\eta^{\mu\nu} = \text{diag}(1, -1, -1, -1)$ ]. They can be expanded in the orthonormal basis (5) as

$$|Z\rangle = \frac{\sum_{m=0}^{\lambda} \sum_{j=0; \frac{1}{2}}^{(\lambda-m)/2} \sum_{q_a, q_b=-j}^j \varphi_{q_a, q_b}^{j, m}(Z) |j, m\rangle_{q_a, q_b}}{\det(\sigma_0 + Z^\dagger Z)^{\lambda/2}}, \quad (12)$$

with coefficients  $\varphi_{q_a, q_b}^{j, m}(Z)$  in (7). Coherent states are normalized,  $\langle Z|Z\rangle = 1$ , but they do not constitute an orthogonal set since they have a non-zero (in general) overlap given by

$$\langle Z'|Z\rangle = \frac{K_\lambda(Z'^\dagger, Z)}{K_{\lambda/2}(Z'^\dagger, Z') K_{\lambda/2}(Z^\dagger, Z)}, \quad (13)$$

with  $K_\lambda$  the Bergmann kernel in (9).

Using orthogonality properties of these homogeneous polynomials, a resolution of unity for isospin- $\lambda$  CS has

been proved in [18], namely  $1 = \int_{\mathbb{G}_2^4} |Z\rangle\langle Z| d\mu(Z, Z^\dagger)$ , with integration measure

$$d\mu(Z, Z^\dagger) = \frac{12d\lambda}{\pi^4} \frac{\prod_{u,v=1}^2 d\text{Re}(z_{uv}) d\text{Im}(z_{uv})}{\det(\sigma_0 + Z^\dagger Z)^4}. \quad (14)$$

Instead of the four complex coordinates  $z_{uv}$ , we shall introduce an alternative parametrization of  $Z$  in terms of eight angles  $\theta_{a,b}, \vartheta_\pm \in [0, \pi)$  and  $\phi_{a,b}, \beta_\pm \in [0, 2\pi)$ , given by the following decomposition

$$Z = V_a \begin{pmatrix} \xi_+ & 0 \\ 0 & \xi_- \end{pmatrix} V_b^\dagger, \quad \xi_\pm = \tan \frac{\vartheta_\pm}{2} e^{i\beta_\pm},$$

$$V_\ell = \begin{pmatrix} \cos \frac{\theta_\ell}{2} & -\sin \frac{\theta_\ell}{2} e^{i\phi_\ell} \\ \sin \frac{\theta_\ell}{2} e^{-i\phi_\ell} & \cos \frac{\theta_\ell}{2} \end{pmatrix}, \quad \ell = a, b, \quad (15)$$

where  $V_{a,b}$  represent rotations in layers  $\ell = a, b$  (note their ‘‘conjugated’’ character). In this coordinate system, the integration measure (14) can be alternatively written as

$$d\mu(Z, Z^\dagger) = \frac{3d\lambda}{2^9\pi^4} (\cos \vartheta_+ - \cos \vartheta_-)^2 d\Omega_+ d\Omega_- d\Omega_a d\Omega_b, \quad (16)$$

where  $d\Omega_\pm = \sin \vartheta_\pm d\vartheta_\pm d\beta_\pm$  and  $d\Omega_\ell = \sin \theta_\ell d\theta_\ell d\phi_\ell$  ( $\ell = a, b$ ) are solid angle elements. Readers acquainted with the Haldane’s sphere picture for the monolayer case can make a comparison between the  $2 \times 2$  complex matrix  $Z$  parametrization (15) and the usual stereographic projection  $z = \tan(\theta/2)e^{i\phi}$  of a point  $(\theta, \phi)$  (polar and azimuthal angles) of the Riemann sphere  $\mathbb{S}^2$  onto the complex plane.

### C. Coherent state expectation values and localization in phase space

Instead of the Fock space realization, it is sometimes more convenient to use a coherent state picture (Bargmann representation) of a general state  $|\psi\rangle \in \mathcal{H}_\lambda(\mathbb{G}_2^4)$  given by the overlap  $\psi(Z) \equiv \langle Z|\psi\rangle$  between  $|\psi\rangle$  and a general CS  $|Z\rangle$  like (12). For example, the Bargmann representation of the basis states  $|\psi\rangle = |q_a, q_b\rangle^{j,m}$  is given in terms of the homogeneous polynomials in (7) as  $\psi(Z) = \varphi_{q_a, q_b}^{j,m}(Z)/K_{\lambda/2}(Z^\dagger, Z)$ .

As an interesting alternative to the bosonic (Schwinger) realization (1) of the  $U(4)$  matrix generators  $\tau_{\mu\nu}$  in Fock space, we can also provide a differential representation of  $\tau_{\mu\nu}$  in the Bergmann space of holomorphic functions  $\phi(Z)$  as follows. Given a  $U(4)$  group element (written in block matrix form)

$$U = \begin{pmatrix} A & B \\ C & D \end{pmatrix}, \quad A, B, C, D \in \text{Mat}(2, \mathbb{C}),$$

a point  $Z$  in the Grassmannian  $\mathbb{G}_2^4 = U(4)/U(2)^2$  can be identified with  $Z = BD^{-1}$  in the chart where  $D$  is invertible. From the composition law of two group elements  $U'' = U'U$  we get the (Möbius-like) transformation

$$Z' = B''D''^{-1} = (A'Z + B')(C'Z + D')^{-1}$$

of  $Z$  under a group translation  $U'$ . For a small  $U(4)$  transformation  $U' = e^{\omega^{\mu\nu}\tau_{\mu\nu}} = I_{4 \times 4} + \omega^{\mu\nu}\tau_{\mu\nu} + O(2)$ , and expanding  $\phi(Z')$  in Taylor (first order) series expansion at  $Z$

$$\phi(Z') = \phi(Z) + \omega^{\mu\nu}\mathcal{T}_{\mu\nu}\phi(Z) + O(2), \quad (17)$$

we obtain the differential realization  $\mathcal{T}_{\mu\nu}$  of the  $U(4)$  generators  $\tau_{\mu\nu}$  on the space of holomorphic functions. For example, it is easy to see that the differential realization of the imbalance ppin generator  $\tau_{k0}/2$  is given by  $\mathcal{P}_3 = z^\mu \partial_\mu - \lambda$ , where  $z^\mu = \text{tr}(Z\sigma_\mu)/2, \mu = 0, 1, 2, 3$  [we use the Einstein summation convention and denote  $\partial_\mu = \partial/\partial z^\mu$  and  $z_\nu = \eta_{\nu\mu}z^\mu$ , with  $\eta_{\nu\mu} = \text{diag}(1, -1, -1, -1)$  the Minkowskian metric]. In addition, spin  $\mathcal{S}_k$  and  $\mathcal{R}_{k3}$  are written in terms of  $\mathcal{M}_{\mu\nu} = z_\mu \partial_\nu - z_\nu \partial_\mu$  as  $\mathcal{S}_i = \frac{i}{2}\epsilon^{ikl}\mathcal{M}_{kl}$  and  $\mathcal{R}_{k3} = \mathcal{M}_{k0}$ , respectively, where  $\epsilon^{ikl}$  is the totally antisymmetric tensor. The explicit expression of the remainder  $U(4)$  differential operators  $\mathcal{T}_{\mu\nu}$  can be seen in [18].

With this differential realization, the (cumbersome) computation of expectation values of operators in a coherent state (usually related to order parameters in the mean-field approximation) is reduced to the (easy) calculation of derivatives of the Bergmann kernel (9) as:

$$\langle Z|T_{\mu\nu}|Z\rangle = K_\lambda^{-1}(Z, Z^\dagger)\mathcal{T}_{\mu\nu}K_\lambda(Z, Z^\dagger). \quad (18)$$

We shall use this simple formula to compute the energy surface (the CS expectation value  $\langle Z|H|Z\rangle$  of the Hamiltonian  $H$ ). For example, in terms of  $M_{\mu\nu} = 2i\lambda \frac{z_\mu \bar{z}^\nu - z_\nu \bar{z}^\mu}{\det(\sigma_0 + Z^\dagger Z)}$ , the CS expectation values of spin and ppin operators turns out to be

$$\begin{aligned} \langle S_1 \rangle &= M_{23}, \quad \langle S_2 \rangle = M_{31}, \quad \langle S_3 \rangle = M_{12}, \\ \langle R_{k3} \rangle &= iM_{0k}, \quad \langle \vec{S} \rangle^2 + \langle \vec{R}_3 \rangle^2 = M_{\mu\nu}M^{\mu\nu}/2, \\ \langle P_1 \rangle &= \lambda \text{Re}[\text{tr}(Z)(1 + \det(Z^\dagger))]/\det(\sigma_0 + Z^\dagger Z), \\ \langle P_3 \rangle &= \lambda(\det(Z^\dagger Z) - 1)/\det(\sigma_0 + Z^\dagger Z), \end{aligned} \quad (19)$$

where  $\text{Re}$  denotes the real part [ $\langle P_2 \rangle$  corresponds to the imaginary part] and  $i$  is the imaginary unit. Note that the following identity for the magnitude of the  $SU(4)$  isospin is automatically fulfilled for coherent state expectation values:

$$\langle \vec{S} \rangle^2 + \langle \vec{P} \rangle^2 + \langle \mathbf{R} \rangle^2 = \lambda^2. \quad (20)$$

For  $\lambda = 1$  it coincides with the variational ground state condition provided in [6]. For BLQH systems at  $\nu = 2/\lambda$  we have seen in [22] that the spin and ppin phases are characterized for maximum values of  $\langle \vec{S} \rangle^2 = \lambda^2$  and  $\langle \vec{P} \rangle^2 = \lambda^2$ , respectively.

As we have already commented, the Husimi function  $Q_\psi(Z)$  of a given state  $|\psi\rangle$  is the CS expectation value  $Q_\psi(Z) = \langle Z|\rho|Z\rangle$  of the corresponding density matrix  $\rho = |\psi\rangle\langle\psi|$  (this definition can be directly extended to mixed states).  $Q_\psi(Z)$  provides the probability of finding  $|\psi\rangle$  in a coherent state  $|Z\rangle$ . For example, for

$|\psi\rangle = |j_a, m_a, j_b, m_b\rangle$  the Husimi function follows a multivariate distribution function [20]. Taking into account the CS closure relation  $1 = \int_{\mathbb{G}_2} |Z\rangle\langle Z| d\mu(Z, Z^\dagger)$  with integration measure (14), we see that  $Q_\psi$  is normalized according to  $\int_{\mathbb{G}_2} Q_\psi(Z) d\mu(Z, Z^\dagger) = 1$  for For unit norm states  $\langle\psi|\psi\rangle = 1$ . An interesting quantity is the Husimi second moment:

$$M_\psi = \int_{\mathbb{G}_2} Q_\psi^2(Z) d\mu(Z, Z^\dagger), \quad (21)$$

which has to do with the so called ‘‘inverse participation ratio’’ (IPR). Broadly speaking, the IPR measures the spread of a state  $|\psi\rangle$  over a basis  $\{|i\rangle\}_{i=1}^d$ . More precisely, if  $p_i$  is the probability of finding the (normalized) state  $|\psi\rangle$  in  $|i\rangle$ , then the IPR is defined as  $M_\psi = \sum_i p_i^2$ . If  $|\psi\rangle$  only ‘‘participates’’ of a single state  $|i_0\rangle$ , then  $p_{i_0} = 1$  and  $M_\psi = 1$  (large IPR), whereas if  $|\psi\rangle$  equally participates on all of them (equally distributed),  $p_i = 1/d, \forall i$ , then  $M_\psi = 1/d$  (small IPR). Therefore, the IPR is a measure of the localization of  $|\psi\rangle$  in the corresponding basis. For our case, the Husimi second moment (21) measures how close is  $|\psi\rangle$  to a coherent state  $|Z\rangle$ . We conjecture that  $M_\psi$  attains its maximum value (maximum localization) when  $|\psi\rangle$  is itself a (minimum uncertainty) CS. We have calculated this maximum value for each  $\lambda$  in [20] and it turns out to be:

$$M_{\max}(\lambda) = \frac{1}{16} - \frac{1/2}{1+\lambda} + \frac{45/32}{1+2\lambda} + \frac{3/32}{3+2\lambda}, \quad (22)$$

which tends to  $M_{\max}(\infty) = 1/16$  for high isospin  $\lambda$  values. This conjecture has been proved for harmonic oscillator CS [34] and spin- $j$  or  $SU(2)$  CS [35]. Here we shall see that the ground state attains this maximum value in spin a ppin phases, thus indicating that it is maximally localized in these phases (see next section). One could also other localization measures like Wehrl’s entropy

$$W_\psi = - \int_{\mathbb{G}_2} Q_\psi(Z) \ln Q_\psi(Z) d\mu(Z, Z^\dagger), \quad (23)$$

which measures the area occupied by  $\psi$  in phase space. However, we shall prefer  $M_\psi$  to  $W_\psi$  since it is easier to compute.

### III. MODEL HAMILTONIAN AND QUANTUM PHASES

In Ref. [22] we have analyzed the ground state structure of BLQH at  $\nu = 2/\lambda$ . The Hamiltonian we used is an adaptation of the Landau-site Hamiltonian for  $\nu = 2$  [6]

$$H = H_C + H_{ZpZ}. \quad (24)$$

which consists of Coulomb and a combination of Zeeman and pseudo-Zeeman interactions. Discarding  $U(4)$ -invariant terms, the Coulomb part

$$H_C = 4\varepsilon_D^- P_3^2 - 2\varepsilon_X^- (\vec{S}^2 + \vec{R}_3^2 + P_3^2), \quad (25)$$

as a sum of the naive capacitance ( $\varepsilon_D^-$ ) and the exchange ( $\varepsilon_X^-$ ) interactions. The exchange and capacitance energy gaps are given in terms of the interlayer distance  $\delta$  by

$$\varepsilon_X^\pm = \frac{1}{4} \sqrt{\frac{\pi}{2}} \left( 1 \pm e^{(\delta/\ell_B)^2/2} \operatorname{erfc} \left( \frac{\delta}{\sqrt{2}\ell_B} \right) \right) \mathcal{E}_C, \quad (26)$$

and  $\varepsilon_D^- = \frac{\delta}{4\ell_B} \mathcal{E}_C$ , where  $\mathcal{E}_C = e^2/(4\pi\epsilon\ell_B)$  is the Coulomb energy unit and  $\ell_B = \sqrt{\hbar c/(eB)}$  the magnetic length. In the following we shall simply put  $\varepsilon_X^- = \varepsilon_X$  and  $\varepsilon_D^- = \varepsilon_D$  as no confusion will arise. We shall usually choose  $\delta = \ell_B$ , which gives  $\varepsilon_X \simeq 0.15$  in Coulomb units (we shall use Coulomb units throughout the article unless otherwise stated). The (pseudo) Zeeman part

$$H_{ZpZ} = -\Delta_Z S_3 - \Delta_t P_1 - \Delta_b P_3 \quad (27)$$

is comprised of: Zeeman ( $\Delta_Z$ ), interlayer tunneling ( $\Delta_t$ , also denoted by  $\Delta_{\text{SAS}}$  in the literature [7]) and bias ( $\Delta_b$ ) gaps. The bias term creates an imbalanced configuration between layers.

For  $\nu = 2/\lambda$  ( $N = 2\lambda$  magnetic flux quanta), Coulomb (two-body) interactions must be renormalized by the number of boson pairs  $N(N-1)$  and one-body interactions by  $N$  to make the energy an intensive quantity. Therefore, the Hamiltonian proposed for arbitrary  $\lambda$  is an adaptation of (24) of the form

$$H_\lambda = \frac{H_C}{N(N-1)} + \frac{H_{ZpZ}}{N}, \quad N = 2\lambda, \quad (28)$$

To study the semiclassical limit, we now replace the operators  $P_j, S_j$  and  $R_{ij}$  by their expectation values (19) in a isospin- $\lambda$  coherent state  $|Z\rangle$ .

A minimization process of the ground state energy surface  $\langle Z|H_\lambda|Z\rangle$  reveals the existence of three quantum phases: spin, canted and ppin, which are characterized by maximum and minimum values of the squared spin  $\langle \vec{S} \rangle$  and squared ppin  $\langle \vec{P} \rangle$  CS expectation values (order parameters). For the sake of simplicity, let us restrict ourselves for this semiclassical analysis to the balanced case (i.e. discard terms proportional to  $\varepsilon_D$  and  $\Delta_b$ ). Using the parametrization (15) of  $Z$ , we found in [22] the common relations

$$\beta_+ = \beta_- = 0, \quad \vartheta_+ + \vartheta_- = \pi, \quad \theta_a + \theta_b = \pi, \quad \phi_a = \phi_b. \quad (29)$$

in all phases. In the spin and ppin phases we have

$$\text{Spin} : \vartheta_+^s = 0 = \theta_a^s, \quad \text{Ppin} : \vartheta_+^p = -\pi/2 = \theta_a^p, \quad (30)$$

respectively. In the canted phase we get the more involved expression

$$\begin{aligned} \tan \vartheta_+^c &= \pm \sqrt{\frac{(\Delta_t^2 - \Delta_Z^2)^2 - (4\Delta_Z \varepsilon_X(\lambda))^2}{-(\Delta_t^2 - \Delta_Z^2)^2 + (4\Delta_t \varepsilon_X(\lambda))^2}}, \quad (31) \\ \tan \theta_b^c &= \mp \frac{\Delta_t}{\Delta_Z} \sqrt{\frac{(\Delta_t^2 - \Delta_Z^2)^2 - (4\Delta_Z \varepsilon_X(\lambda))^2}{-(\Delta_t^2 - \Delta_Z^2)^2 + (4\Delta_t \varepsilon_X(\lambda))^2}}, \end{aligned}$$

where we have defined  $\varepsilon_X(\lambda) = \lambda\varepsilon_X/(2\lambda - 1)$ . The phase transition points (spin-canted and canted-ppin) depend on  $\lambda$  and are located at

$$\begin{aligned}\Delta_t^{\text{sc}}(\lambda) &= \sqrt{\Delta_Z^2 + 4\varepsilon_X(\lambda)\Delta_Z}, \\ \Delta_t^{\text{cp}}(\lambda) &= 2\varepsilon_X(\lambda) + \sqrt{\Delta_Z^2 + 4\varepsilon_X^2(\lambda)}.\end{aligned}\quad (32)$$

For  $\Delta_t < \Delta_t^{\text{sc}}(\lambda)$  the BLQH system at  $\nu = 2/\lambda$  is in the spin phase, for  $\Delta_t^{\text{sc}}(\lambda) \leq \Delta_t \leq \Delta_t^{\text{cp}}(\lambda)$  it is in the canted phase and for  $\text{rashba}\Delta_t > \Delta_t^{\text{cp}}(\lambda)$  it is in the ppin phase [see [22] for more details]. Note that we have two different solutions of  $(\vartheta_+^c, \theta_b^c)$  in the canted phase, given by the signs  $(+, -)$  and  $(-, +)$  in equation (31), leading to the same minimum energy  $\langle Z_\pm^c | H_\lambda | Z_\pm^c \rangle$ , with  $Z_\pm^c = Z(\theta_{a,b}, \phi_{a,b}, \vartheta_\pm, \beta_\pm)|_\pm^c$  the corresponding stationary point in the Grassmannian  $\mathbb{G}_2^4$  for any of the two solutions  $(+) = (+, -)$  and  $(-) = (-, +)$  together with the common restrictions (29). Even though both coherent states  $|Z_+^c\rangle$  and  $|Z_-^c\rangle$  give the same CS energy expectation value  $\langle Z_+^c | H_\lambda | Z_+^c \rangle = \langle Z_-^c | H_\lambda | Z_-^c \rangle$  (see [22]), they are distinct; in fact, they are almost orthogonal  $\langle Z_+^c | Z_-^c \rangle \simeq 0$  in the canted phase. This indicates that the ground state is degenerated and there is a broken symmetry in the thermodynamic limit. Let us study the ground state structure in the phase-space (Bargmann) picture of section II.

#### IV. GROUND STATE ANALYSIS IN PHASE-SPACE AND LOCALIZATION MEASURES

##### A. Variational results

We start with the analysis of the variational ground state. Let us denote collectively by  $Z_+^0$  and  $Z_-^0$  the two sets of stationary points in any of the three (spin, canted and ppin) quantum phases (note that  $Z_+^0 = Z_-^0$  in the spin and ppin phases). A good variational approximation to the true ground state is achieved by taking the normalized symmetric combination

$$|Z_{\text{sym}}^0\rangle = \frac{|Z_+^0\rangle + |Z_-^0\rangle}{\sqrt{2(1 + \text{Re}(\langle Z_+^0 | Z_-^0 \rangle)}}. \quad (33)$$

Using the general expression of the CS overlap (13) and the Bergmann kernel  $K_\lambda(Z'^t, Z) = [1 + \text{tr}(Z'^t Z) + \det(Z'^t Z)]^\lambda$ , we can easily compute the corresponding Husimi function

$$Q_{\text{sym}}^0(Z) = |\langle Z_{\text{sym}}^0 | Z \rangle|^2 = \frac{|\langle Z_+^0 | Z \rangle + \langle Z_-^0 | Z \rangle|^2}{2(1 + \text{Re}(\langle Z_+^0 | Z_-^0 \rangle))}. \quad (34)$$

We shall restrict, for the sake of simplicity, to the plane  $(\vartheta_+, \theta_b)$  of the 8-dimensional Grassmannian phase-space  $\mathbb{G}_2^4$  with constraints (29), where non-trivial angle values

(31) are found in the canted phase. In the plane  $(\vartheta_+, \theta_b)$ , the Husimi function adopts a quite simple form given by

$$Q_{\text{sym}}^0(\vartheta_+, \theta_b) = \frac{(\cos(\vartheta_+ - \vartheta_+^0) + \cos(\theta_b - \theta_b^0))^{2\lambda}}{2^{2\lambda}}, \quad (35)$$

where  $(\vartheta_+^0, \theta_b^0)$  must be replaced by (30) and (31) in the spin, ppin and canted phases, respectively. In Figure 1 we represent a contour plot of  $Q_{\text{sym}}^0(\vartheta_+, \theta_b)$  in the three phases. We see that the variational state is localized around  $(\vartheta_+^s, \theta_b^s) = (0, 0)$  [or equivalently  $(\vartheta_+^s, \theta_b^s) = (\pi, \pi)$ ] in the spin phase, and around  $(\vartheta_+^p, \theta_b^p) = (\pi/2, \pi/2)$  in the ppin phase. In both, spin and ppin, phases we have  $|Z_+^0\rangle = |Z_-^0\rangle$  and therefore  $|Z_{\text{sym}}^0\rangle$  is coherent. In the canted phase, the variational ground state splits into two different packets,  $|Z_+^c\rangle \neq |Z_-^c\rangle$ , localized around the two stationary solutions (31). Both packets have negligible overlap  $\langle Z_+^c | Z_-^c \rangle \simeq 0$  and recombine in the spin and ppin regions. This delocal-

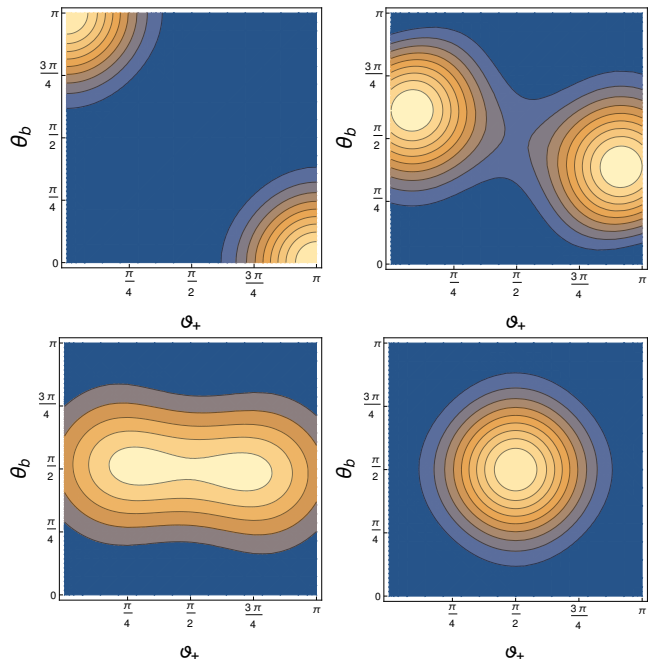


FIG. 1: Contour plot of the Husimi function (34) of the variational ground state in the plane  $(\vartheta_+, \theta_b)$  of the phase-space  $\mathbb{G}_2^4$  for  $\lambda = 3$ , Zeeman  $\Delta_Z = 0.01$ , layer distance  $\delta = \ell_B$  and four values of tunneling gap  $\Delta_t$ . The top-left panel corresponds to the spin phase ( $\Delta_t = 0.01$ ), the top-right and bottom-left panels correspond to the canted phase ( $\Delta_t = 0.1$  and  $\Delta_t = 0.2$ , respectively) and the bottom-right panel corresponds to the canted phase ( $\Delta_t = 0.5$ ). Lighter zones correspond to higher values of the Husimi function, that is, to higher probability for the ground state to be coherent.

ization of  $|Z_{\text{sym}}^0\rangle$  in phase-space inside the canted phase is captured by the Husimi function second moment (21). Indeed, in figure 2 and we represent the localization of the variational and exact (see next section) ground state in phase-space measured by the Husimi second moment

as a function of the tunneling  $\Delta_t$  (we fix  $\Delta_Z = 0.01$  and  $\delta = \ell_B$ ). We compare the two cases:  $\lambda = 1$  and  $\lambda = 3$ . In the spin and ppin phases we have maximum localization [maximum moment (22)], giving  $M_{\max}(1) = 3/10$  and  $M_{\max}(3) = 25/168$ , since the ground state is a (minimal uncertainty) coherent state [note that, in the exact case, the maximum moment value is only attained asymptotically in the ppin phase]. In the transition from the spin to the canted phase we observe a sudden delocalization (a drop of the Husimi second moment) of the ground state wave function in phase-space. Therefore, the canted region is characterized for having a much more delocalized ground state than in the spin and ppin regions. Thus, we conclude that the Husimi second moment serves as an order parameter characterizing the three phases and the phase transition points.

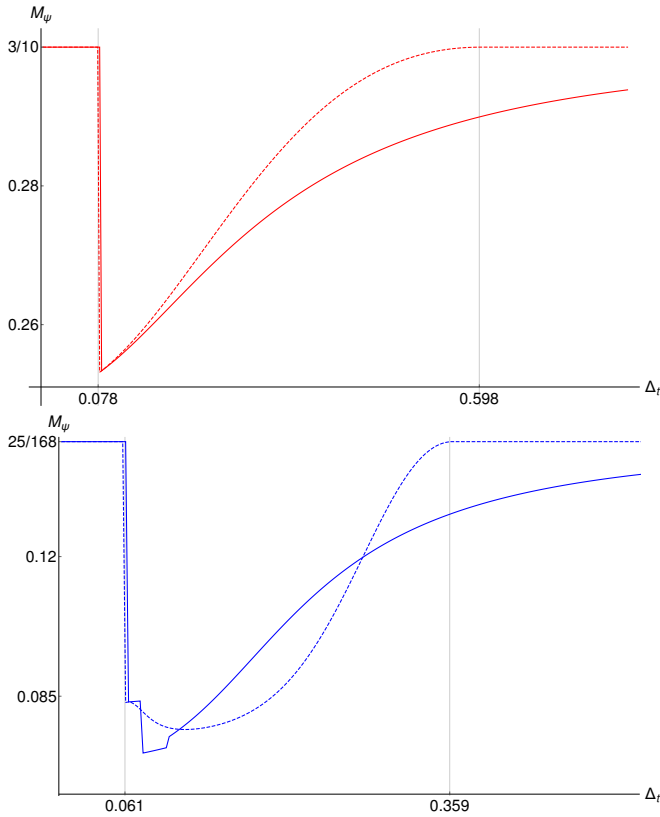


FIG. 2: Second moment  $M_\psi$  of the Husimi function  $Q_\psi$  of the variational (dashed) and exact (solid) ground states  $\psi$  as a function of the tunneling  $\Delta_t$  for Zeeman  $\Delta_Z = 0.01$ , interlayer distance  $\delta = \ell_B$  and  $\lambda = 1$  (top red) and  $\lambda = 3$  (bottom blue). Maximum moments values (22) for  $\lambda = 1$  and  $\lambda = 3$  are  $3/10$  and  $25/168$ , respectively. Spin-canted,  $\Delta_t^{\text{sc}}(1) = 0.078$  and  $\Delta_t^{\text{sc}}(3) = 0.061$ , and canted-ppin,  $\Delta_t^{\text{cp}}(1) = 0.598$  and  $\Delta_t^{\text{cp}}(3) = 0.359$ , phase-transition points (32) are marked by vertical dotted grid lines.

In figure 3 we make a 3-dimensional representation and a contour-plot of  $M_{|Z_{\text{sym}}^0\rangle}$  as a function of tunneling  $\Delta_t$  and Zeeman  $\Delta_Z$  gaps for  $\lambda = 1$  and  $\lambda = 3$  (we take

$\delta = \ell_B$ ). The figure 2 corresponds to a cross-section at  $\Delta_Z = 0.01$ . We see as the valley of  $M_{|Z_{\text{sym}}^0\rangle}$  (delocalized state), represented by darker zones of the contour-plot, captures the canted phase in the  $\Delta_t$ - $\Delta_Z$  control parameter plane. The transition from canted to ppin phase is better marked (sharp) for  $\lambda = 3$  than for  $\lambda = 1$ .

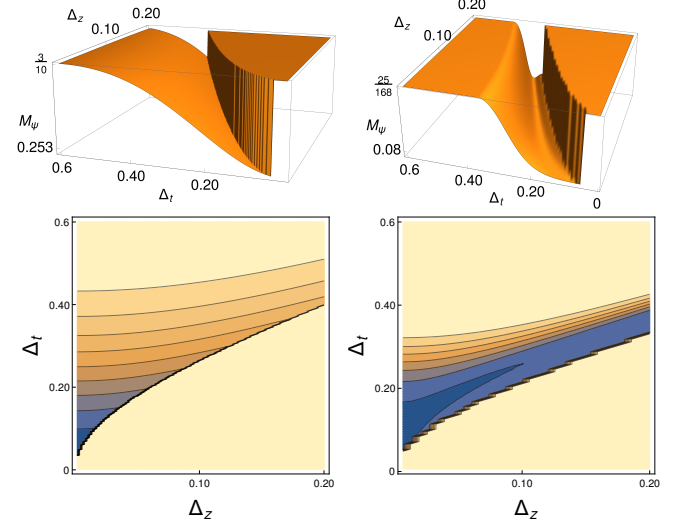


FIG. 3: Second moment of the Husimi function of the variational ground state as a function of tunneling  $\Delta_t$  and Zeeman  $\Delta_Z$  gaps for  $\lambda = 1$  (left) and  $\lambda = 3$  (right). Interlayer distance  $\delta = \ell_B$ . We make a 3D plot (top) and a contour-plot (bottom). The canted phase is characterized by the moment valleys (darker zones of the contour-plot), where the wave function is more delocalized. Spin and ppin phases are characterized by high moment values (lighter zones of the contour-plot), where the wave function is more localized (coherent). The transition from canted to ppin is better marked for  $\lambda = 3$  than for  $\lambda = 1$ .

## B. Numeric diagonalization results

Now we shall diagonalize the Hamiltonian (28) and obtain the corresponding ground state. We shall call it “exact” in contrast to the variational ground state discussed in the previous section. For zero tunneling  $\Delta_t = 0$ , the Hamiltonian is diagonal in the orthonormal basis (5). Its eigenvalues can be straightforwardly obtained from (10) as

$$E_\lambda^{(j,m)}(q_a, q_b) = \frac{\varepsilon_{\text{cap}}(2j + 2m - \lambda)^2 - 8\varepsilon_X j(j + 1)}{2\lambda(2\lambda - 1)} - \frac{\Delta_Z(q_b - q_a) + \Delta_b(2j + 2m - \lambda)}{2\lambda}, \quad (36)$$

where  $\varepsilon_{\text{cap}} = 4\varepsilon_D - 2\varepsilon_X$  denotes the capacitance energy.

Looking at  $E_\lambda^{(j,m)}(q_a, q_b)$ , for small bias  $\Delta_b$ , the lowest energy state must have zero capacitance energy (note that  $\varepsilon_{\text{cap}} \geq 0$ ), that is, it must be balanced  $2j + 2m - \lambda = 0$ . It

must also have maximum angular momentum  $j = \lambda/2 \Rightarrow m = 0$  [remember the constraint  $2j+m \leq \lambda$  in (7)], which gives the minimum exchange energy. Also, the Zeeman energy attains its minimum for  $q_b = \lambda/2 = -qa$ . Therefore, the ground state at  $\Delta_t = 0$  and small  $\Delta_b$  is the basis state  $|\psi_0^s\rangle = |_{-\lambda/2, \lambda/2}^{\lambda/2, 0}\rangle$ , which coincides with the variational CS  $|Z_{\text{sym}}^0\rangle = |Z_+^0\rangle$  in the spin phase. Actually, the ground state in the spin phase is always  $|_{-\lambda/2, \lambda/2}^{\lambda/2, 0}\rangle$ , independent of the control parameters  $(\Delta_t, \Delta_Z, \Delta_b)$ , and the squared spin expectation value is  $\langle \psi_0^s | \vec{S} | \psi_0^s \rangle^2 = \lambda^2$ , thus attaining its maximum value [remember the identity (20)].

For high bias voltage, the dominant part of the energy goes as  $-\Delta_b(2j+2m-\lambda)$  which attains its minimum for  $j=0$  and  $m=\lambda$  (maximum positive imbalance, i.e. all flux quanta in layer  $a$ ). This corresponds to the ppin phase and the ground state in this case is  $|\psi_0^p\rangle = |_{0,0}^{0,\lambda}\rangle$ . This also turns out to be a CS, in fact a particular case of (11) given by

$$|\psi_0^p\rangle = |Z_\infty\rangle = \frac{\det(\mathbf{a}^\dagger)^\lambda |0\rangle_F}{\lambda! \sqrt{\lambda+1}}. \quad (37)$$

The squared ppin expectation value is  $\langle \psi_0^p | \vec{P} | \psi_0^p \rangle^2 = \lambda^2$ , thus attaining its maximum value.

For non-zero tunneling, the Hamiltonian (28) is not diagonal in the orthonormal basis (5). Indeed, the matrix elements of the interlayer tunneling operator are

$$\begin{aligned} P_1 |_{q_a, q_b}^{j, m}\rangle &= C_{q_a, q_b}^{j, m+1} |_{q_a - \frac{1}{2}, q_b - \frac{1}{2}}^{j - \frac{1}{2}, m+1}\rangle + C_{-q_a, -q_b}^{j, m+1} |_{q_a + \frac{1}{2}, q_b + \frac{1}{2}}^{j - \frac{1}{2}, m+1}\rangle + \\ &C_{-q_a + \frac{1}{2}, -q_b + \frac{1}{2}}^{j + \frac{1}{2}, m+2j+2} |_{q_a - \frac{1}{2}, q_b - \frac{1}{2}}^{j + \frac{1}{2}, m}\rangle + C_{q_a + \frac{1}{2}, q_b + \frac{1}{2}}^{j + \frac{1}{2}, m+2j+2} |_{q_a + \frac{1}{2}, q_b + \frac{1}{2}}^{j + \frac{1}{2}, m}\rangle + \\ &C_{q_a, q_b}^{j, m+2j+1} |_{q_a - \frac{1}{2}, q_b - \frac{1}{2}}^{j - \frac{1}{2}, m}\rangle + C_{-q_a + \frac{1}{2}, -q_b + \frac{1}{2}}^{j + \frac{1}{2}, m} |_{q_a - \frac{1}{2}, q_b - \frac{1}{2}}^{j + \frac{1}{2}, m-1}\rangle + \\ &C_{-q_a, -q_b}^{j, m+2j+1} |_{q_a + \frac{1}{2}, q_b + \frac{1}{2}}^{j - \frac{1}{2}, m}\rangle + C_{q_a + \frac{1}{2}, q_b + \frac{1}{2}}^{j + \frac{1}{2}, m} |_{q_a + \frac{1}{2}, q_b + \frac{1}{2}}^{j + \frac{1}{2}, m-1}\rangle, \end{aligned} \quad (38)$$

where the coefficients  $C$  were calculated in [18] and are given by

$$C_{q_a, q_b}^{j, m} = \frac{1}{2} \frac{\sqrt{(j+q_a)(j+q_b)m(\lambda - (m-2))}}{\sqrt{2j(2j+1)}}, \quad j \neq 0, \quad (39)$$

and  $C_{q_a, q_b}^{j, m} = 0$  for  $j=0$ . Taking into account the matrix elements (10) and (38), we can calculate the Hamiltonian matrix elements  $\langle J | H_\lambda | J' \rangle$ , where  $J = \{_{q_a, q_b}^{j, m}\}$  denotes a multi-index running from  $J = 1, \dots, d_\lambda$ . The ground state  $|\psi_0\rangle$  is a linear combination of the basis states  $|J\rangle$  as

$$|\psi_0(\Delta)\rangle = \sum_{J=1}^{d_\lambda} c_J(\Delta) |J\rangle, \quad (40)$$

with coefficients  $c_J(\Delta)$  depending on the Zeeman, tunneling, bias, etc, control parameters (generically denoted by  $\Delta$ ). The Husimi function is then

$$\begin{aligned} Q_{\psi_0(\Delta)}(Z) &= |\langle Z | \psi_0(\Delta) \rangle|^2 \\ &= \sum_{J, J'=1}^{d_\lambda} \frac{\varphi_J(Z) \overline{\varphi_{J'}(Z)}}{\det(\sigma_0 + Z^\dagger Z)^\lambda} c_J(\Delta) \overline{c_{J'}(\Delta)}, \end{aligned} \quad (41)$$

where  $\varphi_J(Z)$  are the homogeneous polynomials (7). The corresponding Husimi function second moment (21) is then given by

$$\begin{aligned} M_{\psi_0}(\Delta) &= \sum_{J, J', K, K'=1}^{d_\lambda} c_J(\Delta) \overline{c_{J'}(\Delta)} c_K(\Delta) \overline{c_{K'}(\Delta)} \\ &\times \int_{\mathbb{G}_2^4} \frac{\varphi_J(Z) \overline{\varphi_{J'}(Z)} \overline{\varphi_K(Z)} \varphi_{K'}(Z)}{\det(\sigma_0 + Z^\dagger Z)^{2\lambda}} d\mu(Z, Z^\dagger). \end{aligned} \quad (42)$$

We have performed a numerical diagonalization of the Hamiltonian (28) for  $\lambda = 1$  (dimension  $d_1 = 6$ ) and  $\lambda = 3$  (dimension  $d_3 = 50$ ) using a mesh of 300 points, with a resolution of tunneling gap  $\Delta_t = 0.5$  in figure 2, and a mesh of  $100 \times 30$  points, with a resolution of  $\Delta_t = 0.6$  and  $\Delta_Z = 0.2$  in the 3D figure 5. The multiple integrals in the 8-dimensional Grassmannian  $\mathbb{G}_2^4$  are also calculated numerically. They are computationally quite hard calculations. In figure 2 we compare variational (dashed curves) with exact (solid curves) values of the Husimi function second moment of the ground state. We see that the variational approximation agrees with the exact calculation in the spin phase and captures quite well the delocalization of the ground state in phase space inside the canted region. In the ppin region, both the variational and exact ground states become again localized although, in the exact case, the maximum moment value is only attained asymptotically for high  $\Delta_t$ . This agreement between variational and exact ground states is also patent when comparing figure 1 with 4 and figure 3 with 5. The variational result captures quite faithfully the ground state structure and localization measures in the three phases.

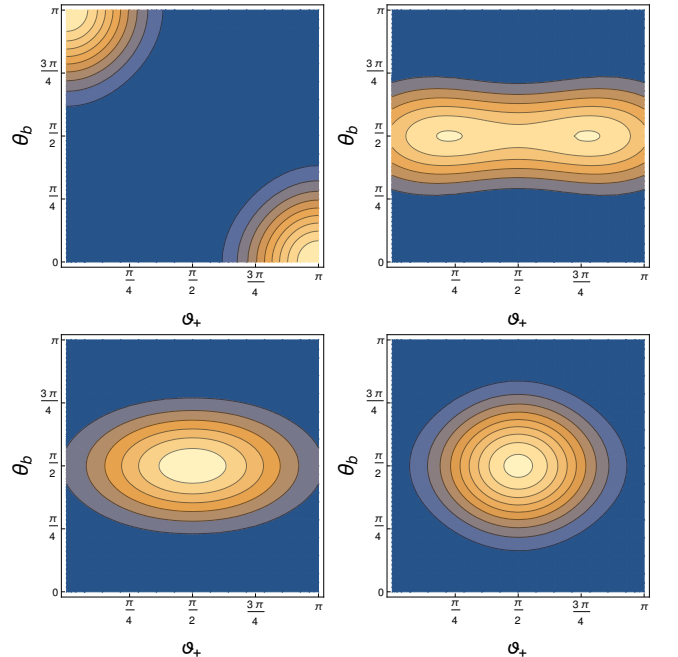


FIG. 4: Contour plot of the Husimi function  $Q_{\psi_0}$  of the exact ground state  $|\psi_0\rangle$  in the plane  $(\vartheta_+, \theta_b)$  of the phase-space  $\mathbb{G}_2^4$  for  $\lambda = 3$ . Same structure and values as in the variational case of figure 1.



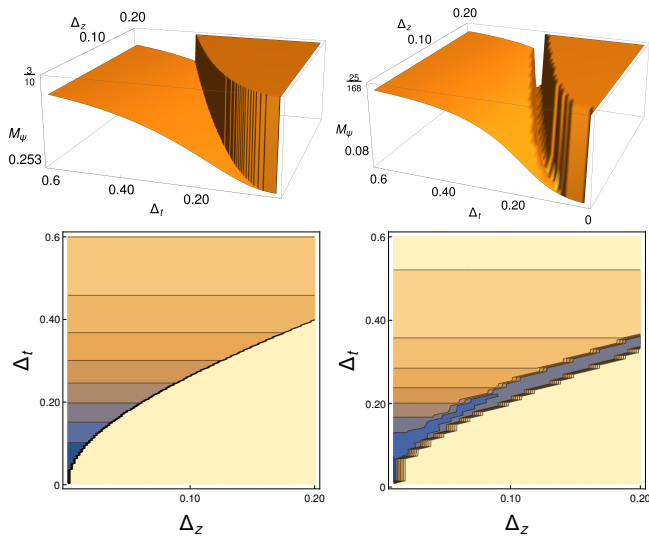


FIG. 5: Second moment of the Husimi function of the exact ground state as a function of tunneling  $\Delta_t$  and Zeeman  $\Delta_Z$  for  $\lambda = 1$  (left) and  $\lambda = 3$  (right). Same structure and values as in the variational case of figure 3.

In the analytical (variational) study developed in section III, we have restricted ourselves to the balanced case, for the sake of simplicity. To finish, and for the sake of completeness, we study the effect of a non-zero bias voltage (non-balanced case) on the exact ground state  $\psi$  Husimi second moment  $M_\psi$ . In figure 6 we represent contour-plots of  $M_\psi$  as a function of tunneling  $\Delta_t$  and Zeeman  $\Delta_Z$  for  $\lambda = 3$  and two values of bias voltage:  $\Delta_b = 0.5$  and  $\Delta_b = 1$ . We see that a non-zero  $\Delta_b$  modifies the spin-canted and canted-ppin phase transition points as regards the balanced case (32), here given by transitions from high to low momentum  $M_\psi$ . Therefore, the canted region, characterized by low momentum  $M_\psi$  (darker zones in the contour-plot), moves in the phase diagram  $\Delta_t$ - $\Delta_Z$  when varying  $\Delta_b$ . In particular, the second moment analysis also reproduces the already noticed fact that the ppin phase dominates at higher values of  $\Delta_b$ .

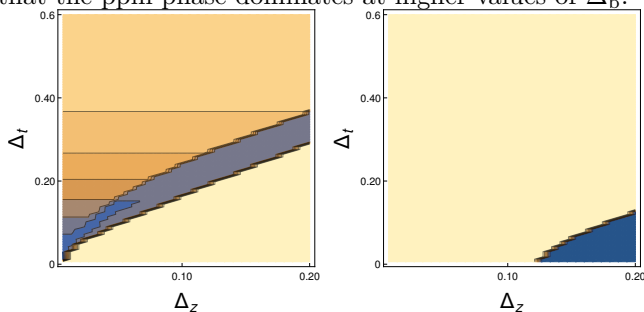


FIG. 6: Second moment of the Husimi function of the exact ground state as a function of tunneling  $\Delta_t$  and Zeeman  $\Delta_Z$  for  $\lambda = 3$ ,  $\delta = \ell_B$  and bias voltage  $\Delta_b = 0.5$  (left) and  $\Delta_b = 1$  (right). For higher  $\Delta_b$ , the ppin phase dominates more and more in the phase diagram  $\Delta_Z$ - $\Delta_t$ .

## V. CONCLUSIONS

Using a coherent state representation of the ground state  $\psi$ , in the Grassmannian phase space  $\mathbb{G}_2^4$ , given by the Husimi  $Q_\psi$  function, we have characterized the three quantum phases (spin, ppin and canted) of BLQH system models at fractional filling factors  $\nu = 2/\lambda$ . We have found that the Husimi function second moment quantifies the localization (inverse volume) of  $\psi$  in phase space and serves as an order parameter distinguishing the spin and ppin phases (high localization) from the canted phase (low localization). Otherwise stated, the ground state in spin and ppin phases is highly coherent, whereas in the canted phase it is a kind of Schrödinger cat, i.e., a superposition of two (quasi-)orthogonal coherent states. We have also visualized the ground state Husimi function in the spin, ppin and canted phases using two-dimensional cross-sections of the 8-dimensional Grassmannian phase space  $\mathbb{G}_2^4$ . The variational (analytic) treatment produces good qualitative and quantitative results as regards the exact (numeric) diagonalization calculations.

We believe that this coherent state picture of BLQH systems provides an alternative and useful tool and a new perspective compared to more traditional approaches to the subject. In fact, this picture can be extended to more general  $N$ -component fractional quantum Hall systems and some steps in this direction have already been done [21].

## Acknowledgements

The work was supported by the project FIS2014-59386-P (Spanish MINECO and European FEDER funds). C. Peón-Nieto acknowledges the research contract with Ref. 4537 financed by the project above. We all are grateful to Emilio Pérez-Romero for his valuable collaboration at the early stages of this work.

- [1] P.W. Anderson, Absence of Diffusion in Certain Random Lattices, *Phys. Rev.* 109, 1492 (1958).
- [2] F. Wegner, Inverse Participation Ratio in  $2 + \epsilon$  Dimensions, *Z. Phys. B* 36, 209 (1980)
- [3] T. Brandes, S. Kettemann, Anderson Localization and Its Ramifications: Disorder, Phase Coherence and Electron Correlations, *Lecture Notes in Physics* 630, Springer 2003
- [4] C. Aulbach, A. Wobst, G.-L. Ingold, P. Hanggi, and I. Varga, Phase-space visualization of a metal-insulator transition, *New J. Phys.* 6, 70 (2004).
- [5] F. Evers and A. D. Mirlin, Anderson transitions, *Rev. Mod. Phys.* 80, 1355 (2008)
- [6] Z.F. Ezawa, M. Eliashvili, G. Tsitsishvili, Ground-state structure in  $\nu = 2$  bilayer quantum Hall systems. *Phys. Rev.* B71 (2005) 125318
- [7] Z. F. Ezawa, *Quantum Hall Effects: Field Theoretical Approach and Related Topics*, 2nd Edition (World Scientific, Singapore 2008)
- [8] A. H. MacDonald, R. Rajaraman and T. Jungwirth, Broken-symmetry ground states in  $\nu = 2$  bilayer quantum Hall systems, *Phys. Rev. B* 60, 8817 (1999)
- [9] L. Brey, E. Demler and S. Das Sarma, Electromodulation of the Bilayered  $\nu = 2$  Quantum Hall Phase Diagram, *Phys. Rev. Lett.* 83 (1999) 168-171
- [10] J. Schliemann A. H. MacDonald, Bilayer Quantum Hall Systems at Filling Factor  $\nu = 2$ : An Exact Diagonalization Study, *Phys. Rev. Lett.* 84 (2000) 4437.
- [11] K. Hasebe and Z. F. Ezawa, Grassmannian fields and doubly enhanced Skyrmions in the bilayer quantum Hall system at  $\nu = 2$ , *Phys. Rev.* B66, 155318 (2002)
- [12] A. Fukuda, A. Sawada, S. Kozumi, D. Terasawa, Y. Shimoda, Z. F. Ezawa, N. Kumada, and Y. Hirayama, Magnetotransport study of the canted antiferromagnetic phase in bilayer  $\nu = 2$  quantum Hall state, *Phys. Rev.* B73 (2006) 165304
- [13] F.D.M. Haldane, Fractional Quantization of the Hall Effect: A Hierarchy of Incompressible Quantum Fluid States, *Phys. Rev. Lett.* 51 (1983) 605-608
- [14] J.R. Klauder and Bo-Sture Skagerstam, *Coherent States: Applications in Physics and Mathematical Physics*, World Scientific (1985)
- [15] A. Perelomov, *Generalized Coherent States and Their Applications*, Springer-Verlag (1986)
- [16] J-P. Gazeau, *Coherent States in Quantum Physics*, Wiley-VCH, Berlin, 2009.
- [17] S.T. Ali, J.-P. Antoine, J.-P. Gazeau, *Coherent States, Wavelets and Their Generalizations*, Springer, second edition (2014).
- [18] M. Calixto and E. Pérez-Romero, Coherent states on the Grassmannian  $U(4)/U(2)^2$ : Oscillator realization and bilayer fractional quantum Hall systems, *J. Phys. A: Math. Theor.* 47, (2014) 115302.  
Erratum: there is a misprint in equation (49) of this reference. One must replace  $C_{\cdot, \cdot}^{:, 2j+m+1}$  by  $C_{\cdot, \cdot}^{:, 2j+m+2}$ .
- [19] M. Calixto and E. Pérez-Romero, Interlayer coherence and entanglement in bilayer quantum Hall states at filling factor  $\nu = 2/\lambda$ , *J. Phys.: Condens. Matter* 26 (2014) 485005
- [20] M. Calixto and E. Pérez-Romero, Some properties of Grassmannian  $U(4)/U(2)^2$  coherent states and an entropic conjecture, *J. Phys. A: Math. Theor.* 48 (2015) 495304
- [21] M. Calixto, C. Peón-Nieto and E. Pérez-Romero, Coherent states for N-component fractional quantum Hall systems and their nonlinear sigma models, *Annals of Physics* 373 (2016) 52-66
- [22] M. Calixto, C. Peon-Nieto and E. Perez-Romero, Hilbert space and ground state structure of bilayer quantum Hall systems at  $\nu = 2/\lambda$ , *Phys. Rev. B*95 (2017) 235302. DOI: 10.1103/PhysRevB.95.235302, arXiv:1703.05021v2
- [23] U. Leonhardt, *Measuring the Quantum State of Light*, New York: Cambridge University Press (1997)
- [24] Gerhard Kirchmair, Brian Vlastakis, Zaki Leghtas, Simon E. Nigg, Hanhee Paik, Eran Ginossar, Mazyar Mirrahimi, Luigi Frunzio, S. M. Girvin and R. J. Schoelkopf, Observation of quantum state collapse and revival due to the single-photon Kerr effect, *Nature* 495, 205-209 (2013). doi:10.1038/nature11902
- [25] F. J. Arranz, Z. S. Safi, R. M. Benito, and F. Borondo, Zeros of the Husimi function and quantum numbers in the HCP molecule, *Eur. Phys. J. D* 60, 279 (2010).
- [26] F. J. Arranz, L. Seidel, C. G. Giralda, R. M. Benito, and F. Borondo, Onset of quantum chaos in molecular systems and the zeros of the Husimi function, *Phys. Rev. E* 87, 062901 (2013).
- [27] D. Weinmann, S. Kohler, G.-L. Ingold, and P. Hänggi, Disordered systems in phase space, *Ann. Phys. (Leipzig)* 8, SI277 (1999).
- [28] M. Calixto and E. Romera, Identifying topological-band insulator transitions in silicene and other 2D gapped Dirac materials by means of Rényi-Wehrl entropy, *EPL*, 109 (2015) 40003
- [29] E. Romera, R. del Real, and M. Calixto, Husimi distribution and phase-space analysis of a Dicke-model quantum phase transition, *Phys. Rev. A* 85, 053831 (2012).
- [30] M. Calixto, R. del Real and E. Romera, Husimi distribution and phase-space analysis of a vibron-model quantum phase transition, *Phys. Rev. A* 86, 032508 (2012).
- [31] O. Castaños, M. Calixto, F. Pérez-Bernal and E. Romera, Identifying the order of a quantum phase transition by means of Wehrl entropy in phase space, *Phys. Rev. E* 92, 052106 (2015)
- [32] E. Romera, O. Castaños, M. Calixto and F. Pérez-Bernal, Delocalization properties at isolated avoided crossings in Lipkin-Meshkov-Glick type Hamiltonian models, *J. Stat. Mech.* 013101 (2017)
- [33] C. Pérez-Campos, J.R. González-Alonso, O. Castaños, R. López-Peña, Entanglement and Localization of a Two-Mode Bose-Einstein Condensate, *Annals of Physics* 325, 325-344 (2010)
- [34] A. Wehrl, On the relation between classical and quantum mechanical entropies, *Rep. Math. Phys.* 16 353 (1979)
- [35] E. H. Lieb and J. P. Solovej, Proof of an entropy conjecture for Bloch coherent spin states and its generalizations, *Acta Math.* 212, 379 (2014).
- [36] J.K. Jain, *Composite fermions*, Cambridge University Press, New York, 2007.
- [37] I. Affleck, The quantum Hall effects,  $\sigma$ -models at  $\theta = \pi$  and quantum spin chains, *Nucl. Phys.* B257 (1985) 397; I. Affleck, Exact critical exponents for quantum spin chains, non-linear  $\sigma$ -models at  $\theta = \pi$  and the quantum

- hall effect, B265 (1986) 409-447;
- I. Affleck, Critical behaviour of  $SU(n)$  quantum chains and topological non-linear  $\sigma$ -models, Nucl. Phys. B305 (1988), 582-596
- [38] N. Read and S. Sachdev, Some features of the phase diagram of the square lattice  $SU(N)$  antiferromagnet, Nucl. Phys. B316 (1989) 609
- [39] D. P. Arovas, A. Karlhede and D. Lilliehöök,  $SU(N)$  quantum Hall skyrmions, Phys. Rev. B59 (1999) 13147-13150.
- [40] L.C. Biedenharn, J.D. Louck, Angular Momentum in Quantum Physics, Addison-Wesley, Reading, MA, 1981; L.C. Biedenharn, J.D. Louck, The Racah-Wigner Algebra in Quantum Theory, Addison-Wesley, New York, MA 1981